PatchAD: Patch-based MLP-Mixer for Time Series Anomaly Detection

Zhijie Zhong¹, Zhiwen Yu¹, Yiyuan Yang², Weizheng Wang³ and Kaixiang Yang^{1*}

¹South China University of Technology ²University of Oxford ³City University of Hong Kong

csemor@mail.scut.edu.cn, zhwyu@scut.edu.cn, yiyuan.yang@cs.ox.ac.uk, weizheng.wang@ieee.org, yangkx@scut.edu.cn,

Abstract

Anomaly detection stands as a crucial aspect of time series analysis, aiming to identify abnormal events in time series samples. The central challenge of this task lies in effectively learning the representations of normal and abnormal patterns in a labellacking scenario. Previous research mostly relied on reconstruction-based approaches, restricting the representational abilities of the models. In addition, most of the current deep learning-based methods are not lightweight enough, which prompts us to design a more efficient framework for anomaly detection. In this study, we introduce PatchAD, a novel multi-scale patch-based MLP-Mixer architecture that leverages contrastive learning for representational extraction and anomaly detection. Specifically, PatchAD is composed of four distinct MLP Mixers, exclusively utilizing the MLP architecture for high efficiency and lightweight architecture. Additionally, we also innovatively crafted a dual project constraint module to mitigate potential model degradation. Comprehensive experiments demonstrate that PatchAD achieves state-of-the-art results across multiple real-world multivariate time series datasets. Our code is publicly available. ¹

1 Introduction

Time series anomaly detection is a pivotal aspect of data analysis, focused on identifying abnormal patterns within timeseries data that significantly deviate from normal behavior [Belay et al., 2023; Choi et al., 2021]. This process becomes more complex in multivariate temporal anomaly detection, where it involves multiple channel dimensions. Driven by the rapid progression of large-scale sensing technologies and enhanced data storage capabilities, temporal anomaly detection has found widespread application in various sectors. For instance, in the field of the Internet of Things (IoT), it serves to monitor abnormal events in sensor data [Yang et al., 2021]. In healthcare sector, it plays a vital role in monitoring a person's

physiological data, thereby assisting in the early detection of health problems [Cook *et al.*, 2020].

However, extracting anomalies from extensive and complex temporal data presents significant challenges. First, accurately defining the representations of anomalies is difficult due to the varied and evolving nature of real-world anomalies. For instance, anomalies in machinery could manifest as either high or fluctuating temperatures under different scenarios. Second, labels for anomalous events in time-series data are probably absent or hard to acquire. Thirdly, the high dimensionality and temporal dependencies inherent in time-series data are intricate. While the typical approach involves classifying different time points as normal or anomalous, relying solely on a single time point is often not feasible.

Due to the powerful representational capacity of neural networks, numerous deep learning-based techniques [Munir et al., 2019; Zhang et al., 2022] have been proposed for time series anomaly detection, demonstrating remarkable performance and attracting significant interest from the research community. While supervised and semi-supervised methods grapple with the scarcity of labeled data, unsupervised techniques [Zhou et al., 2019; Su et al., 2019] have gained prominence due to their ability to operate without strict labeling requirements. While [Xu et al., 2022] designed six different anomaly injection methods to train the model in a self-supervised approach, [Carmona et al., 2021] utilized outlier exposure and mixup to construct a self-supervised task.

Reconstruction-based approaches, as typical and common unsupervised methods, involve learning representations of historical data and identifying samples that cannot be accurately reconstructed during testing as anomalies [Park *et al.*, 2018]. This approach has experienced rapid development due to its clear concept and its proficiency in managing complex data representations. However, due to their robust reconstruction capabilities, these methods excel at recovering anomalous data, posing a challenge for reconstruction-based approaches. The core issue is the ineffectiveness of these methods in distinctly modeling normal and abnormal data, complicating their ability to accurately identify anomalies.

Recently, contrastive learning has been captivated by its straightforward, yet exceptional performance, proving effective in areas such as computer vision [Chen *et al.*, 2020]. In time series anomaly detection, several methods have begun incorporating contrastive learning to enhance model repre-

^{*}Corresponding author

¹https://github.com/EmorZz1G/PatchAD

sentational capabilities. Nonetheless, these approaches often overlook the design of network structures tailored for contrastive learning. They either do not explicitly model interchannel dependencies [Yang et al., 2023] or rely solely on basic MLPs or Transformers that focus on temporal information [Zhou et al., 2022], mainly considering point-level features [Audibert et al., 2020]. Nevertheless, poor training and inference speeds, architectural complexity, and a lack of lightweight features are some of the drawbacks of high-performing techniques. It was recently shown by [Zeng et al., 2022] that MLP structures can also result in outstanding performance on time series tasks. Additionally, they neglected the model degradation issue in contrastive learning, meaning models might degrade or collapse during the training process.

In this paper, we propose <u>PatchAD</u>, a novel <u>Patchbased MLP</u> architecture designed for time series <u>Anomaly Detection</u>. PatchAD leverages contrastive learning to tackle the complexities of time series anomaly detection. Inspired by [Yang et al., 2023], we hypothesize that normal time series points share similar latent patterns, indicating a strong correlation among normal time points. On the contrary, anomalies struggle to establish connections with other anomaly points or normal points. Hence, normal data exhibits consistent representations across different views, while anomalies struggle to maintain consistent representations. This underlying principle forms the core of our approach to anomaly detection.

Specifically, we introduce a novel Multi-scale Patching and Embedding approach. This method decomposes the input data along the temporal dimension into non-overlapping patches, enabling the model to learn from features that contain richer semantic information, moving beyond simple point-level features. To address various time scales, different submodels are utilized, each focusing on different patch sizes. To capture diverse views of temporal data representation, we propose different Patch Mixer Encoders to learn the mixed relationships among inter-patches, intra-patches, and inter-channel connections. We utilize a shared MixRep Mixer to uniformly represent the feature space. To prevent the degradation, we not only construct diverse encoders but also introduce a Dual Project Constraint mechanism to prevent the model from settling on overly simplistic solutions, thus substantially boosting its representational capabilities.

The main contributions of our proposed PatchAD can be summarized as follows:

- The novel PatchAD model, innovatively structured on contrastive learning framework, is adept at managing diverse anomaly types. This is achieved by creating Interpatch Encoders and Intra-patch Encoders, which generate both inter-patch and intra-patch perspectives.
- Employing a strategy named Multi-scale Patching and Embedding, PatchAD integrates multi-scale subsequence modules constructed exclusively with MLPs. This design is intended to facilitate the learning of semantically richer features.
- Dual Project Constraint mechanism is specifically designed to impose constraints on the model, reducing its susceptibility to simple, trivial solutions and thus increasing its expressive power.

 PatchAD's efficacy is underscored by comprehensive experimental results on eight datasets. These results highlight its superior performance compared to the SOTA time series anomaly detection methods.

2 Preliminaries

In this section, we provide an initial exposition on the formal representation of time series anomaly detection, related methods, and contrastive learning. These are the foundational elements of the research problem and serve as the motivation for our work.

2.1 Problem Formulation

In this paper, we consider a multivariate time series of length T in an unsupervised setting:

$$\mathcal{X} = (x_1, x_2, \cdots, x_T),\tag{1}$$

where $x_t \in \mathbb{R}^C$ represents a C-dimensional channel feature, such as data from C sensors or machines. The objective is to train a model using \mathcal{X}_{train} and provide predictions $\mathcal{Y}_{test} = (y_1, y_2, \cdots, y_{T'})$ on another sequence \mathcal{X}_{test} of length T'. Here, $y_t \in \{0, 1\}$, where 1 signifies an anomaly at that time point and 0 indicates a normal point.

2.2 Time Series Anomaly Detection

There exist various methods proposed for time series anomaly detection, encompassing statistical approaches, classical machine learning methods, and deep learning techniques. Statistical methods involve moving averages and the autoregressive integrated moving average (ARIMA) model. Classical machine learning methods encompass classificationbased approaches like One-Class Support Vector Machine (OCSVM) [Schölkopf et al., 2001] and Support Vector Data Description (SVDD) [Tax and Duin, 2004]. Deep learning methods include DAGMM, OmniAnomaly [Su et al., 2019], USAD [Audibert et al., 2020], LSTM-VAE [Park et al., 2018], and DeepAnT, which are trained on normal data and detect anomalies by inference using reconstruction errors. Some techniques [Kim et al., 2023],[Chen et al., 2022] have leveraged self-attention mechanisms and have demonstrated promising detection results. Recognizing the limitations imposed by the reconstruction-based assumption, research efforts like [Li et al., 2021a] introduced sequence variational autoencoder model based on smoothness constraints, whereas [Xu et al., 2021] proposed prior and sequence associations for temporal modeling, both achieving enhanced performance.

2.3 MLP Mixer for Time Series

The MLP Mixer, initially proposed as a novel architecture for computer vision [Tolstikhin *et al.*, 2021], has gained significant attention in recent years. Recently, there has been analysis indicating that MLP Mixers can effectively handle sequential data and find applications in other domains, such as time series prediction. Specifically, works like [Nie *et al.*, 2023; Gong *et al.*, 2023] have focused on prediction tasks, particularly for multi-step time series prediction, leveraging the capabilities of MLP Mixers to achieve improved forecasting re-

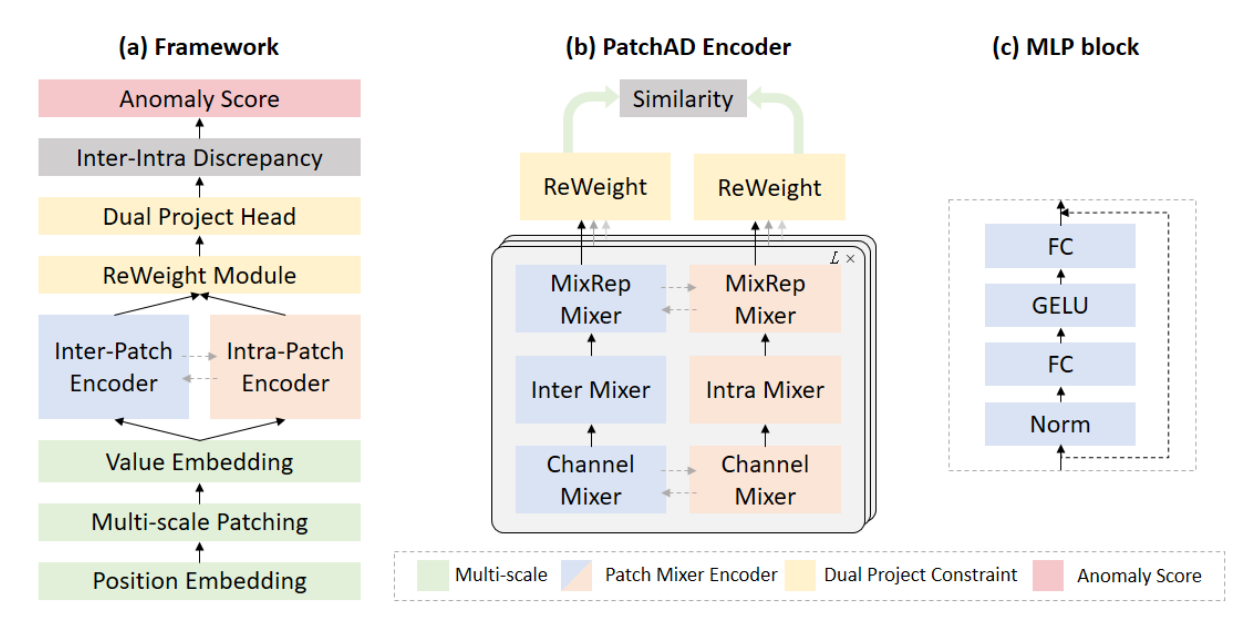


Figure 1: The workflow of the proposed PatchAD framework.

sults. Their experiments demonstrate that the MLP Mixer surpasses existing Transformer-based and LSTM-based methods in long sequence time-series forecasting (LSTF). To the best of our knowledge, there is currently an absence of MLP Mixer application in the time series anomaly detection.

2.4 Contrastive Learning

Contrastive learning has garnered considerable attention across various domains for its capacity to train models by contrasting positive pairs against negative ones. The objective is to drive the model to bring positive pairs closer together in the learned representation space while pushing apart negative pairs. Additionally, methods like BYOL [Grill et al., 2020] and SimSiam [Chen and He, 2021] have demonstrated advanced performance without explicitly constructing negative pairs. Recently, studies such as [Eldele et al., 2021] and [Pranavan et al., 2022] have explored the integration of contrastive learning into time series analysis. [Yang et al., 2023], on the other hand, combines self-attention with contrastive learning, achieving state-of-the-art results in time series anomaly detection.

3 Proposed Method

3.1 Overall Architecture

Figure 1 illustrates the overall structure of PatchAD. PatchAD adopts patch sizes at multiple scales. We exemplify its architecture using a single scale. PatchAD is an *L*-layer network, where each layer comprises distinct modules: MLP Mixers, Project head, and ReWeight, forming its structure. We have devised four distinct types of MLP Mixers: Channel Mixer, Inter Mixer, Intra Mixer, and MixRep Mixer, each dedicated to learning various channels, inter-patch, intra-patch relationships, and a unified representation space. The Project head serves to prevent the model from converging to trivial so-

lutions, while the ReWeight module manages the weights across different layers.

The focal point of our design lies in the four distinct MLP Mixers. Inspired by [Yang *et al.*, 2023], we utilize various MLP Mixers to learn different representations from the input. Normal points share a common latent space across different views, while anomalies, being scarce and lacking specific patterns, struggle to share a coherent representation with normal points. Consequently, normal points exhibit minor discrepancies across different views, whereas anomalies showcase larger variations. PatchAD leverages inter-intra discrepancy to model this relationship.

3.2 Multi-scale Patching and Embedding

To enhance the temporal contextual representation in time series, we incorporated Transformer positional encoding. Acknowledging the significance of different sequence lengths in the time series analysis, we introduced *Multi-scale Patching* in PatchAD. This enables PatchAD to focus on features of varying sequence lengths. Moreover, incorporating multiscale information helps compensate for information loss during the patching process. The input data with C channels and length T is transformed into patches of size P. It can be seen as dividing the time series data into N nonoverlapping blocks of patches, which is called $Patching(\cdot)$. Thus, the original data of dimensions $C \times T$ is transformed into $C \times N \times P$.

$$\mathcal{X} = \text{Patching}(\text{PE}(\mathcal{X})), \ \mathcal{X}^{C \times T} \to \mathcal{X}^{C \times N \times P},$$
 (2)

where $PE(\cdot)$ is positional embedding.

PatchAD employs two value embeddings, i.e., $VE(\cdot)$, facilitating the features from two distinct perspectives within the framework. And $VE(\cdot)$ is a single linear layer.

$$\mathcal{X}_{inter} = VE(\mathcal{X}), \ \mathcal{X}^{C \times N \times P} \to \mathcal{X}^{C \times N \times D},$$

$$\mathcal{X}_{intra} = VE(\mathcal{X}), \ \mathcal{X}^{C \times N \times P} \to \mathcal{X}^{C \times P \times D}.$$
(3)

3.3 Patch Mixer Encoder

PatchAD comprises L layers of Patch Mixer layers. This encoder incorporates four distinct MLP Mixers to extract features across different dimensions. Figure 1(c) illustrates the MLP block we designed. It consists of two fully connected layers, a normalization layer, a GELU non-linear activation layer, and utilizes a residual connection from input to output. This can be represented as:

$$\mathcal{X} = FC(GELU(FC(Norm(\mathcal{X})))) + \mathcal{X}. \tag{4}$$

The following are the different types of MLP Mixers utilized in PatchAD:

- 1. *The Channel Mixer* enables PatchAD to capture correlations among different channels.
- 2. *The Inter Mixer* empowers PatchAD to capture interpatch representations, facilitating the learning of global expressions.
- The Intra Mixer enables PatchAD to capture intra-patch representations, facilitating the learning of local expressions.
- 4. *The MixRep Mixer* allows PatchAD to embed two distinct views into the same representation space.

The diagram depicts PatchAD comprised of an inter-patch encoder and an intra-patch encoder, generating representations denoted as $\mathcal{N} \in \mathbb{R}^{C \times N \times D}$ and $\mathcal{P} \in \mathbb{R}^{C \times P \times D}$, representing the inter-patch and intra-patch views, respectively. It's important to note that *The Channel Mixer* and *The MixRep Mixer* share weights, while *The Inter Mixer* and *The Intra Mixer* have their own weights. This design facilitates PatchAD in learning differences between views and prevents model degradation.

3.4 Dual Project Constraint

To prevent the model from converging to trivial solutions, each layer's output requires to be constrained by *Dual Project Head*. Prior research suggests that employing a similar structure effectively prevents models from converging to trivial solutions. For instance, SimCLR [Chen *et al.*, 2020] uses a projection head that maps augmented views of an image into a latent space and promotes smoother convergence during training. The projection head comprises two layers of MLP connections, excluding non-linear and normalization layers. Hence, for both the inter-patch and intra-patch encoders, we can derive the projected representations $\mathcal{N}' \in \mathbb{R}^{C \times N \times D}$ and $\mathcal{P}' \in \mathbb{R}^{C \times P \times D}$. This computation can be represented as:

$$\mathcal{N}' = FC(FC(\mathcal{N})), \ \mathcal{P}' = FC(FC(\mathcal{P})). \tag{5}$$

To amalgamate outputs from different layers and prevent model degradation, we employ a simple ReWeight module to assign distinct weights to various layers. Considering representations from L layers, $\{\mathcal{N}_1, \mathcal{N}_2, \cdots, \mathcal{N}_L\}$ and $\{\mathcal{P}_1, \mathcal{P}_2, \cdots, \mathcal{P}_L\}$, we can derive the final result:

$$\mathcal{N}_{l} = \alpha_{l} \cdot \mathcal{N}_{l}, \ \alpha_{l} = \operatorname{Softmax}(\alpha),
\mathcal{P}_{l} = \beta_{l} \cdot \mathcal{P}_{l}, \ \beta_{l} = \operatorname{Softmax}(\beta).$$
(6)

The introduction of ReWeight allows for a better balance between outputs from different layers, resulting in improved performance.

3.5 Objective Function

The inter-patch encoder and intra-patch encoder can represent two distinct views, denoted as $\mathcal N$ and $\mathcal P$. To quantify the dissimilarity between these representations, we utilize a comparative loss function based on Kullback–Leibler divergence (KL divergence), termed as Inter-Intra Discrepancy. Given the scarcity of anomalies in the data and the abundance of normal samples sharing hidden patterns, similar inputs should yield similar representations for both.

The loss function for \mathcal{N} and \mathcal{P} can be defined as follows:

$$\mathcal{L}_{\mathcal{N}}\{\mathcal{P}, \mathcal{N}\} = \sum_{i} \mathrm{KL}(\mathcal{N}, \mathrm{StopGrad}(\mathcal{P})) + \mathrm{KL}(\mathrm{StopGrad}(\mathcal{P}), \mathcal{N}),$$
(7)

$$\mathcal{L}_{\mathcal{P}}\{\mathcal{P}, \mathcal{N}\} = \sum_{i} \mathrm{KL}(\mathcal{P}, \mathrm{StopGrad}(\mathcal{N})) + \mathrm{KL}(\mathrm{StopGrad}(\mathcal{N}), \mathcal{P}),$$
(8)

where $KL(\cdot||\cdot)$ represents the KL divergence distance, and StopGrad denotes gradient stoppage, employed for asynchronously optimizing the two branches. The combined loss is defined as:

$$\mathcal{L}_{cont} = \frac{\mathcal{L}_{\mathcal{N}} - \mathcal{L}_{\mathcal{P}}}{len(\mathcal{N})}.$$
 (9)

Due to the mismatch in dimensions between $\mathcal N$ and $\mathcal P$, an initial upsampling of both is required for comparability. For the inter-patch view, where only differences between patches exist, we replicate the final $\mathcal N$ within patches. Conversely, for the intra-patch view, exhibiting anomalies between points within patches, we replicate it multiple times to obtain the final $\mathcal P$. This also addresses the necessity for introducing multi-scale, as it compensates for the information loss during upsampling.

To prevent model degradation, we augment the original loss function with an additional constraint from the projection head, defined as:

$$\mathcal{L}_{proj} = \frac{\mathcal{L}_{\mathcal{N}'} - \mathcal{L}_{\mathcal{P}}}{len(\mathcal{N})} + \frac{\mathcal{L}_{\mathcal{N}} - \mathcal{L}_{\mathcal{P}'}}{len(\mathcal{N})}.$$
 (10)

The final PatchAD loss consists of the aforementioned two components, with a constraint coefficient used to control the strength of the constraint:

$$\mathcal{L} = (1 - c) \cdot \mathcal{L}_{cont} + c \cdot \mathcal{L}_{proj}. \tag{11}$$

3.6 Anomaly Score

Based on the assumption that normal points across different views share hidden patterns, while anomalies exhibit larger discrepancies, the difference between the two views can be employed as an anomaly score. The final anomaly score can be expressed as:

$$\label{eq:anomalyScore} {\rm AnomalyScore}(\mathcal{X}) = \sum {\rm KL}(\mathcal{N},\mathcal{P}) + {\rm KL}(\mathcal{P},\mathcal{N}). \ \ (12)$$

Based on the aforementioned anomaly score, we set a hyperparameter σ to determine whether a point is considered an anomaly. If it surpasses the threshold, it is identified as an outlier.

$$y_i = \begin{cases} 1, \text{ AnomalyScore}(\mathcal{X}_i) \ge \sigma \\ 0, \text{ AnomalyScore}(\mathcal{X}_i) < \sigma. \end{cases}$$
 (13)

Table 1: Comprehensive comparative results on four datasets. The P, R and F1 are the precision, recall and F1-score. All results are in %, the best ones are in **Bold**, and the second ones are underlined.

Dataset		MSL			SMAP			PSM			SWaT		Average
Metric	P	R	F1	F1									
OCSVM [Schölkopf et al., 2001]	59.78	86.87	70.82	53.85	59.07	56.34	62.75	80.89	70.67	45.39	49.22	47.23	61.27
IForest [Liu et al., 2008]	53.94	86.54	66.45	52.39	59.07	55.53	76.09	92.45	83.48	49.29	44.95	47.02	63.12
LOF [Breunig et al., 2000]	47.72	85.25	61.18	58.93	56.33	57.60	57.89	90.49	70.61	72.15	65.43	68.62	64.50
U-Time [Perslev et al., 2019]	57.20	71.66	63.62	49.71	56.18	52.75	82.85	79.34	81.06	46.20	87.94	60.58	64.50
ITAD [Shin et al., 2020]	69.44	84.09	76.07	82.42	66.89	73.85	72.80	64.02	68.13	63.13	52.08	57.08	68.78
DAGMM [Zong et al., 2018]	89.60	63.93	74.62	86.45	56.73	68.51	93.49	70.03	80.08	89.92	57.84	70.40	73.40
VAR [Anderson, 1976]	74.68	81.42	77.90	81.38	53.88	64.83	90.71	83.82	87.13	81.59	60.29	69.34	74.80
MMPCACD [Yairi et al., 2017]	81.42	61.31	69.95	88.61	75.84	81.73	76.26	78.35	77.29	82.52	68.29	74.73	75.93
CL-MPPCA [Tariq et al., 2019]	73.71	88.54	80.44	86.13	63.16	72.88	56.02	99.93	71.80	76.78	81.50	79.07	76.05
TS-CP2 [Deldari et al., 2021]	86.45	68.48	76.42	87.65	83.18	85.36	82.67	78.16	80.35	81.23	74.10	77.50	79.91
BeatGAN [Zhou et al., 2019]	89.75	85.42	87.53	92.38	55.85	69.61	90.30	93.84	92.04	64.01	87.46	73.92	80.78
LSTM-VAE [Park et al., 2018]	85.49	79.94	82.62	92.20	67.75	78.10	73.62	89.92	80.96	76.00	89.50	82.20	80.97
BOCPD [Adams and MacKay, 2007]	80.32	87.20	83.62	84.65	85.85	85.24	80.22	75.33	77.70	89.46	70.75	79.01	81.39
Deep-SVDD [Ruff et al., 2018]	91.92	76.63	83.58	89.93	56.02	69.04	95.41	86.49	90.73	80.42	84.45	82.39	81.44
LSTM [Hundman et al., 2018]	85.45	82.50	83.95	89.41	78.13	83.39	76.93	89.64	82.80	86.15	83.27	84.69	83.71
OmniAnomaly [Su et al., 2019]	89.02	86.37	87.67	92.49	81.99	86.92	88.39	74.46	80.83	81.42	84.30	82.83	84.56
InterFusion [Li et al., 2021b]	81.28	92.70	86.62	89.77	88.52	89.14	83.61	83.45	83.52	80.59	85.58	83.01	85.57
THOC [Shen et al., 2020]	88.45	90.97	89.69	92.06	89.34	90.68	88.14	90.99	89.54	83.94	86.36	85.13	88.76
AnomalyTrans [Xu et al., 2021]	91.92	96.03	93.93	93.59	99.41	96.41	96.94	97.81	97.37	89.79	100.0	94.62	95.58
DCdetector [Yang et al., 2023]	92.22	97.48	94.77	94.43	98.41	96.38	97.19	98.08	97.63	93.25	100.0	96.51	96.32
PatchAD (Ours)	92.05	98.20	95.02	94.49	99.13	96.75	97.72	98.52	98.11	93.28	100.0	96.52	96.60

Table 2: Overall results on NIPS-TS datasets. All results are in %, the best ones are in **Bold**, and the second ones are underlined.

Dataset	NIE	PS-TS-SV	VAN	NIPS	S-TS-GE	CCO	Average
Metric	P	R	F1	P	R	F1	F1
MatrixProfile [Yeh et al., 2016]	16.70	17.50	17.10	4.60	18.50	7.40	12.25
GBRT [Elsayed et al., 2021]	44.70	37.50	40.80	17.50	14.00	15.60	28.20
LSTM-RNN [Bontemps et al., 2016]	52.70	22.10	31.20	34.30	27.50	30.50	30.85
Autoregression [Rousseeuw and Leroy, 2005]	42.10	35.40	38.50	39.20	31.40	34.90	36.70
OCSVM [Schölkopf et al., 2001]	47.40	49.80	48.50	18.50	74.30	29.60	39.05
IForest* [Liu et al., 2008]	40.60	42.50	41.60	39.20	31.50	39.00	40.30
AutoEncoder [Sakurada and Yairi, 2014]	49.70	52.20	50.90	42.40	34.00	37.70	44.30
AnomalyTrans [Xu et al., 2021]	90.70	47.40	62.30	25.70	28.50	27.00	44.65
IForest [Liu et al., 2008]	56.90	59.80	58.30	43.90	35.30	39.10	48.70
AnomalyTrans [Xu et al., 2021]	90.71	47.43	62.29	29.96	48.63	37.08	49.69
DCdetector [Yang et al., 2023]	96.57	59.08	73.31	38.41	59.73	46.76	60.04
PatchAD (Ours)	96.75	59.15	73.41	40.62	62.88	49.35	61.38

4 Experiments

4.1 Setups and Evaluation Metrics

We applied eight datasets for evaluation: (1) MSL (2) SMAP ²(3) PSM (4) SMD ³ (5) SWaT ⁴ (6) WADI ⁵ (7) NIPS-TS-SWAN (8) NIPSTS-GECCO ⁶. Details about these datasets are outlined in Table 4 in Appendix. Also, implementation and pseudo-code Algorithm 1 details in Appendix.

We compared our model with 27 benchmark models, including: (1) Reconstruction-based; (2) Autoregression-based; (3) Density-based; (4) Clustering-based; (5) Classic methods; (6) Change point detection and time-series segmentation methods; (7) Transformer-based methods; See details in Table 1 and Table 2, or in Appendix 5.

Additionally, we employed various evaluation metrics for assessing, encompassing commonly used metrics in time-

series anomaly detection such as accuracy, precision, recall, and F1-score [Xu et al., 2021]. Moreover, we adopted stateof-the-art evaluation techniques like affiliation precision and affiliation recall [Huet et al., 2022], along with Volume under the surface (VUS) [Paparrizos et al., 2022]. Although the F1-score is a widely used metric, it does not effectively evaluate anomalous events. Therefore, we introduce the following two new metrics. Affiliation precision and recall are evaluation metrics based on the proximity of predicted events to the true labels. VUS considers the inclusion of anomalous events in its evaluation by computing the receiver operator characteristic (ROC) curve. Employing various methodologies allows for a more comprehensive evaluation of our model. To fairly compare with other methods, we utilized the point adjustment technique, identifying an anomalous segment if the model detects any anomaly point within the segment.

4.2 Comparison Results

Data Source Clarification: Due to substantial device variations, to ensure fair comparison with anomaly transformer (AnomalyTrans) and DCdetector, all results mentioned in the paper concerning them are obtained through our reimplementation of their codes. The results of AnomalyTrans and DCdetector in Table 1 and Table 2 are our reproductions.

From Table 1, PatchAD achieves the best average-level F1 performance. As far as we know, there is ongoing controversy regarding the evaluation of time series anomaly detection. However, precision, recall, and F1-score remain the most widely used evaluation metrics. To comprehensively assess the performance of our approach, additional metrics such as affiliation precision/recall and VUS have been introduced.

In Table 2, the NIPS-TS-SWAN and NIPS-TS-GECCO datasets represent more challenging datasets, encompassing a wider array of anomaly types. PatchAD consistently achieves SOTA results on these two datasets compared to other base-

²MSL & SMAP: https://github.com/ML4ITS/mtad-gat-pytorch

³https://github.com/NetManAIOps/OmniAnomaly

⁴https://itrust.sutd.edu.sg/itrust-labs_datasets

⁵https://itrust.sutd.edu.sg/testbeds/water-distribution-wadi

⁶Others: github.com/DAMO-DI-ML/KDD2023-DCdetector

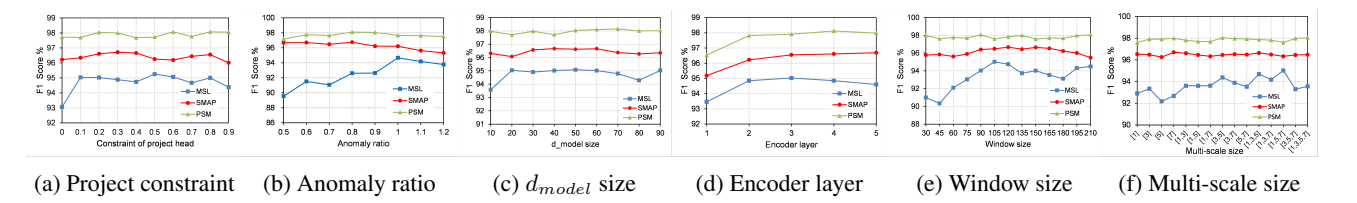


Figure 2: Parameter sensitivity studies of main hyper-parameters in PatchAD.

Table 3: Ablation experiments on MSL, SMAP, WADI datasets.

Dataset		MSL				SM	AP			W	ADI	
Methods	Acc	P	R	F1	Acc	P	R	F1	Acc	P	R	F1
wo_ch_sharing	98.78	91.93	96.90	94.35	98.84	93.50	97.75	95.58	98.71	84.99	94.25	89.38
wo_ch_mixer	98.78	92.03	96.82	94.36	98.77	93.50	97.10	95.27	98.92	85.40	97.93	91.24
wo_pos_emb	97.85	91.51	87.73	89.58	96.47	92.18	79.13	85.16	98.23	83.96	85.53	84.74
wo_constraint	98.51	91.67	94.49	93.06	99.01	93.55	99.05	96.22	98.73	85.26	94.25	89.53
Ours	98.92	92.05	98.20	95.02	99.10	94.45	98.75	96.55	99.06	85.92	100.00	92.43

line methods. Particularly noteworthy is the 9.3% increase in F1-score over the DCdetector and a 24.9% increase over the Anomaly Transformer on the NIPS-TS-GECCO dataset.

Given the remarkable performance of AnomalyTrans and DCdetector surpassing other baselines significantly, we conducted a comprehensive comparison of PatchAD with them across all datasets using multiple metrics, as depicted in Table 5 in Appendix. Our proposed method outperforms or at least remains competitive compared to these two SOTA methods. PatchAD attains superior results across multiple datasets and multiple metrics. Despite PatchAD's relatively simple network structure, its performance remains competitive.

4.3 Model Analysis

Ablation Studies

To study the impact of different components in our model, we conducted ablation experiments across three datasets, as presented in Table 3. The 'wo_ch_sharing' method employs two independent Channel Mixer modules to model channel features, while 'wo_ch_mixer' denotes the removal of the Channel Mixer module. These two variants exhibit significant effects, particularly on the MSL and SMAP datasets, indicating that modeling inter-channel information and sharing channel information are beneficial for model learning. Besides, 'wo_pos_emb' represents a variant without positional encoding, and removing positional encoding significantly affects PatchAD, highlighting the crucial role of positional encoding in its design. Furthermore, 'wo_constraint' showcases the impact of removing the constraint on the projection head. In conjunction with Figure 4a, we observed that a certain level of constraint facilitates easier model optimization, leading to improved results. This constraint prevents the model from converging to trivial solutions. In subsequent experiments, the default setting for the projection head constraint is 0.2.

Parameter Sensitivity

We conducted a sensitivity analysis on PatchAD's parameters. The default parameter settings remain consistent with the basic configuration. Figure 2a demonstrates the impact of the projection head constraint on PatchAD. Overall, it holds more significance for smaller-scale datasets like MSL. However, excessively strong constraints hinder the model's learn-

ing process. Therefore, setting this constraint between 0.1 to 0.4 is more advisable. Figure 2b analyzes PatchAD's final model performance when the anomaly threshold σ ranges from 0.5 to 1.2. The selection of the anomaly threshold appears more robust on the PSM and SMAP datasets compared to the MSL dataset. For most datasets, setting this value between 0.8 and 1 yields optimal results. Figure 2c illustrates how the model's performance is influenced by the network dimension d_{model} . PatchAD demonstrates better results with smaller d_{model} sizes. Therefore, to strike a balance between model performance and complexity, we set $d_{model} = 40$ to ensure PatchAD operates effectively. Figure 2d indicates that PatchAD's performance is influenced by the number of encoder layers, and given a compromise, we set it to 3 or 4. Figure 2e demonstrates PatchAD's robustness concerning the window size, which ranges from 60 to 210. The time window is a critical parameter, typically set to an initial value of 105 across most datasets. Lastly, Figure 2f displays PatchAD's performance under different multi-scale patch size combinations. The outcomes suggest that combining various patch sizes can enhance PatchAD's performance.

Visual Analysis

We visualized PatchAD's response to various anomalies in Figure 3. Synthetic univariate time series were generated by [Lai *et al.*, 2021], incorporating anomalies such as global point anomalies, contextual point anomalies, and pattern anomalies such as seasonal, group, and trend-based anomalies. The first row depicts the original data, while the second row displays PatchAD's output of anomaly scores against the anomaly threshold. In particular, PatchAD has the ability to detect various types of anomalies.

Time Cost

We conducted a time consumption analysis on the SMD dataset under identical experimental conditions. Figure 4b demonstrates that under different sliding step conditions, our method outperforms DCdetector. Specifically, when the step is set to 1, PatchAD's speed is 1.45x faster than DCdetector. Additionally, Figure 4d illustrates the time required for model training with a fixed window size (window size=105). This indicates that PatchAD exhibits higher efficiency in training compared to DCdetector. Figure 4c shows the time required for model training with a fixed sliding step (step=35) while varying the window size from 35 to 175 for different d_{model} sizes. Both graphs show that the time consumption of PatchAD exhibits a linear growth with respect to the independent variables. Thus, increasing the window size or enlarging d_{model} has a relatively minor impact on PatchAD. However,

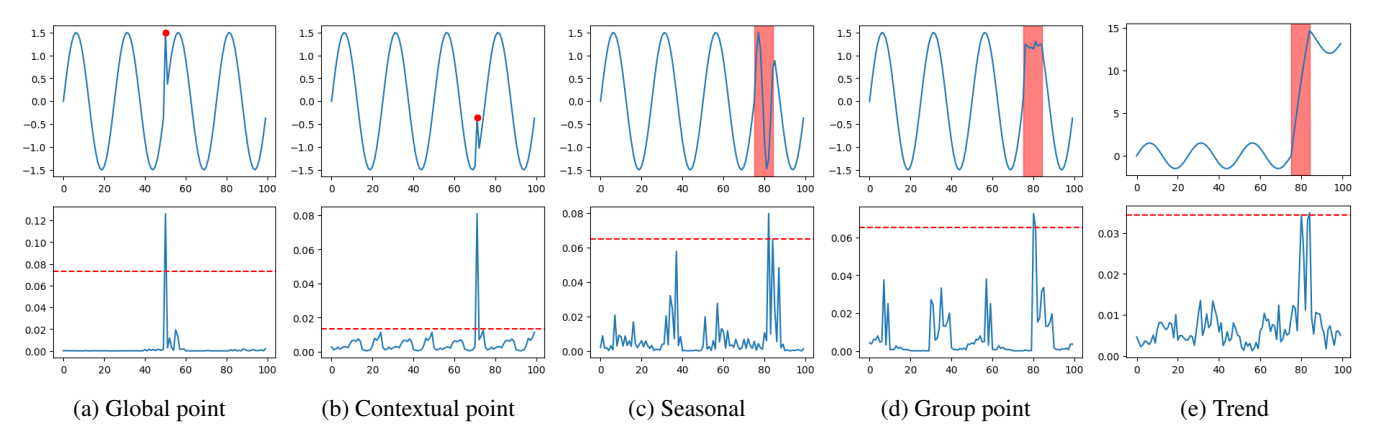


Figure 3: Visualization of generated synthetic data, PatchAD anomaly scores and ground truth.

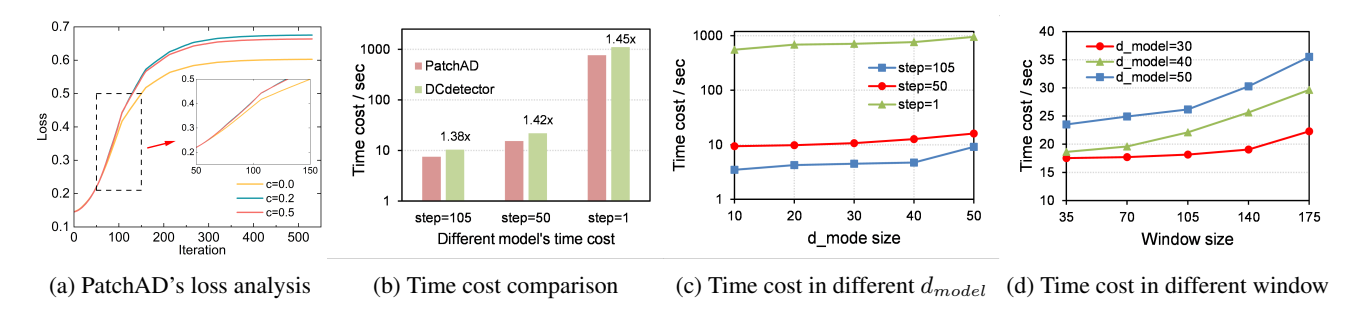


Figure 4: The analysis of PatchAD and DCdetector.

the time step noticeably affects the duration as this parameter leads to increased data volume.

5 Conclusion

We presents PatchAD, an innovative algorithm tailored for time series anomaly detection. PatchAD developed a multiscale, patch-based MLP Mixer architecture grounded in contrastive learning. This architecture is unique in its use of a purely MLP-based approach to discern both inter-patch and intra-patch relationships in time series sequences. By amplifying the differences between two data views, PatchAD enhance its capability to differentiate between normal and anomalous patterns. Furthermore, PatchAD adeptly learns the relationships between different data channels and incorporates a Dual Project Constraint to avert model degradation. Moreover, the efficacy of PatchAD, including its various components, is validated through extensive experimentation. The results demonstrate that proposed PatchAD outperforms other methods across eight benchmark datasets.

References

[Adams and MacKay, 2007] Ryan Prescott Adams and David JC MacKay. Bayesian online changepoint detection. *arXiv* preprint arXiv:0710.3742, 2007.

[Anderson, 1976] Oliver D Anderson. Time-series. 2nd edn., 1976.

[Audibert et al., 2020] Julien Audibert, Pietro Michiardi, Frédéric Guyard, Sébastien Marti, and Maria A. Zuluaga.

USAD: UnSupervised Anomaly Detection on Multivariate Time Series. In *Proceedings of the 26th ACM SIGKDD International Conference on Knowledge Discovery & Data Mining*, pages 3395–3404, Virtual Event CA USA, 2020. ACM.

[Belay et al., 2023] Mohammed Ayalew Belay, Sindre Stenen Blakseth, Adil Rasheed, and Pierluigi Salvo Rossi. Unsupervised Anomaly Detection for IoT-Based Multivariate Time Series: Existing Solutions, Performance Analysis and Future Directions. Sensors, 23(5):2844, 2023.

[Bontemps et al., 2016] Loic Bontemps, Van Loi Cao, James McDermott, and Nhien-An Le-Khac. Collective anomaly detection based on long short-term memory recurrent neural networks. In Future Data and Security Engineering: Third International Conference, FDSE 2016, Can Tho City, Vietnam, November 23-25, 2016, Proceedings 3, pages 141–152. Springer, 2016.

[Breunig et al., 2000] Markus M Breunig, Hans-Peter Kriegel, Raymond T Ng, and Jörg Sander. Lof: identifying density-based local outliers. In *Proceedings of the 2000 ACM SIGMOD international conference on Management of data*, pages 93–104, 2000.

[Carmona *et al.*, 2021] Chris U. Carmona, François-Xavier Aubet, Valentin Flunkert, and Jan Gasthaus. Neural contextual anomaly detection for time series, July 2021.

- [Chen and He, 2021] Xinlei Chen and Kaiming He. Exploring simple siamese representation learning. In *Proceedings of the IEEE/CVF conference on computer vision and pattern recognition*, pages 15750–15758, 2021.
- [Chen et al., 2020] Ting Chen, Simon Kornblith, Mohammad Norouzi, and Geoffrey Hinton. A simple framework for contrastive learning of visual representations. In *International conference on machine learning*, pages 1597–1607. PMLR, 2020.
- [Chen et al., 2022] Zekai Chen, Dingshuo Chen, Xiao Zhang, Zixuan Yuan, and Xiuzhen Cheng. Learning Graph Structures with Transformer for Multivariate Time Series Anomaly Detection in IoT. *IEEE Internet of Things Journal*, 9(12):9179–9189, 2022. arXiv:2104.03466 [cs, eess].
- [Choi *et al.*, 2021] Kukjin Choi, Jihun Yi, Changhwa Park, and Sungroh Yoon. Deep Learning for Anomaly Detection in Time-Series Data: Review, Analysis, and Guidelines. *IEEE Access*, 9:120043–120065, 2021.
- [Cook et al., 2020] Andrew A. Cook, Goksel Misirli, and Zhong Fan. Anomaly Detection for IoT Time-Series Data: A Survey. IEEE Internet of Things Journal, 7(7):6481–6494, 2020.
- [Deldari *et al.*, 2021] Shohreh Deldari, Daniel V Smith, Hao Xue, and Flora D Salim. Time series change point detection with self-supervised contrastive predictive coding. In *Proceedings of the Web Conference 2021*, pages 3124–3135, 2021.
- [Eldele *et al.*, 2021] Emadeldeen Eldele, Mohamed Ragab, Zhenghua Chen, Min Wu, Chee Keong Kwoh, Xiaoli Li, and Cuntai Guan. Time-Series Representation Learning via Temporal and Contextual Contrasting, 2021. arXiv:2106.14112 [cs].
- [Elsayed *et al.*, 2021] Shereen Elsayed, Daniela Thyssens, Ahmed Rashed, Hadi Samer Jomaa, and Lars Schmidt-Thieme. Do we really need deep learning models for time series forecasting? *arXiv preprint arXiv:2101.02118*, 2021.
- [Gong *et al.*, 2023] Zeying Gong, Yujin Tang, and Junwei Liang. PatchMixer: A Patch-Mixing Architecture for Long-Term Time Series Forecasting, 2023.
- [Grill et al., 2020] Jean-Bastien Grill, Florian Strub, Florent Altché, Corentin Tallec, Pierre Richemond, Elena Buchatskaya, Carl Doersch, Bernardo Avila Pires, Zhaohan Guo, Mohammad Gheshlaghi Azar, et al. Bootstrap your own latent-a new approach to self-supervised learning. Advances in neural information processing systems, 33:21271–21284, 2020.
- [Huet et al., 2022] Alexis Huet, Jose Manuel Navarro, and Dario Rossi. Local evaluation of time series anomaly detection algorithms. In *Proceedings of the 28th ACM SIGKDD Conference on Knowledge Discovery and Data Mining*, pages 635–645, 2022.
- [Hundman *et al.*, 2018] Kyle Hundman, Valentino Constantinou, Christopher Laporte, Ian Colwell, and Tom Soderstrom. Detecting spacecraft anomalies using lstms

- and nonparametric dynamic thresholding. In *Proceedings of the 24th ACM SIGKDD international conference on knowledge discovery & data mining*, pages 387–395, 2018
- [Kim et al., 2023] Jina Kim, Hyeongwon Kang, and Pilsung Kang. Time-series anomaly detection with stacked Transformer representations and 1D convolutional network. Engineering Applications of Artificial Intelligence, 120:105964, 2023.
- [Lai et al., 2021] Kwei-Herng Lai, Daochen Zha, Junjie Xu, Yue Zhao, Guanchu Wang, and Xia Hu. Revisiting time series outlier detection: Definitions and benchmarks. In Thirty-fifth conference on neural information processing systems datasets and benchmarks track (round 1), 2021.
- [Li et al., 2021a] Longyuan Li, Junchi Yan, Haiyang Wang, and Yaohui Jin. Anomaly Detection of Time Series With Smoothness-Inducing Sequential Variational Auto-Encoder. IEEE Transactions on Neural Networks and Learning Systems, 32(3):1177–1191, 2021. Conference Name: IEEE Transactions on Neural Networks and Learning Systems.
- [Li et al., 2021b] Zhihan Li, Youjian Zhao, Jiaqi Han, Ya Su, Rui Jiao, Xidao Wen, and Dan Pei. Multivariate time series anomaly detection and interpretation using hierarchical inter-metric and temporal embedding. In Proceedings of the 27th ACM SIGKDD conference on knowledge discovery & data mining, pages 3220–3230, 2021.
- [Liu *et al.*, 2008] Fei Tony Liu, Kai Ming Ting, and Zhi-Hua Zhou. Isolation forest. In 2008 eighth ieee international conference on data mining, pages 413–422. IEEE, 2008.
- [Munir *et al.*, 2019] Mohsin Munir, Shoaib Ahmed Siddiqui, Andreas Dengel, and Sheraz Ahmed. DeepAnT: A Deep Learning Approach for Unsupervised Anomaly Detection in Time Series. *IEEE Access*, 7:1991–2005, 2019.
- [Nie *et al.*, 2023] Yuqi Nie, Nam H. Nguyen, Phanwadee Sinthong, and Jayant Kalagnanam. A Time Series is Worth 64 Words: Long-term Forecasting with Transformers, 2023.
- [Paparrizos et al., 2022] John Paparrizos, Paul Boniol, Themis Palpanas, Ruey S Tsay, Aaron Elmore, and Michael J Franklin. Volume under the surface: a new accuracy evaluation measure for time-series anomaly detection. *Proceedings of the VLDB Endowment*, 15(11):2774–2787, 2022.
- [Park et al., 2018] Daehyung Park, Yuuna Hoshi, and Charles C Kemp. A multimodal anomaly detector for robot-assisted feeding using an lstm-based variational autoencoder. *IEEE Robotics and Automation Letters*, 3(3):1544–1551, 2018.
- [Perslev et al., 2019] Mathias Perslev, Michael Jensen, Sune Darkner, Poul Jørgen Jennum, and Christian Igel. U-time: A fully convolutional network for time series segmentation applied to sleep staging. Advances in Neural Information Processing Systems, 32, 2019.

- [Pranavan *et al.*, 2022] Theivendiram Pranavan, Terence Sim, Arulmurugan Ambikapathi, and Savitha Ramasamy. Contrastive predictive coding for Anomaly Detection in Multi-variate Time Series Data, 2022.
- [Rousseeuw and Leroy, 2005] Peter J Rousseeuw and Annick M Leroy. *Robust regression and outlier detection*. John wiley & sons, 2005.
- [Ruff et al., 2018] Lukas Ruff, Robert Vandermeulen, Nico Goernitz, Lucas Deecke, Shoaib Ahmed Siddiqui, Alexander Binder, Emmanuel Müller, and Marius Kloft. Deep one-class classification. In *International conference on* machine learning, pages 4393–4402. PMLR, 2018.
- [Sakurada and Yairi, 2014] Mayu Sakurada and Takehisa Yairi. Anomaly detection using autoencoders with non-linear dimensionality reduction. In *Proceedings of the MLSDA 2014 2nd workshop on machine learning for sensory data analysis*, pages 4–11, 2014.
- [Schölkopf *et al.*, 2001] Bernhard Schölkopf, John C Platt, John Shawe-Taylor, Alex J Smola, and Robert C Williamson. Estimating the support of a high-dimensional distribution. *Neural computation*, 13(7):1443–1471, 2001.
- [Shen et al., 2020] Lifeng Shen, Zhuocong Li, and James Kwok. Timeseries anomaly detection using temporal hierarchical one-class network. Advances in Neural Information Processing Systems, 33:13016–13026, 2020.
- [Shin et al., 2020] Youjin Shin, Sangyup Lee, Shahroz Tariq, Myeong Shin Lee, Okchul Jung, Daewon Chung, and Simon S Woo. Itad: integrative tensor-based anomaly detection system for reducing false positives of satellite systems. In *Proceedings of the 29th ACM international conference on information & knowledge management*, pages 2733–2740, 2020.
- [Su et al., 2019] Ya Su, Youjian Zhao, Chenhao Niu, Rong Liu, Wei Sun, and Dan Pei. Robust anomaly detection for multivariate time series through stochastic recurrent neural network. In *Proceedings of the 25th ACM SIGKDD international conference on knowledge discovery & data mining*, pages 2828–2837, 2019.
- [Tariq et al., 2019] Shahroz Tariq, Sangyup Lee, Youjin Shin, Myeong Shin Lee, Okchul Jung, Daewon Chung, and Simon S Woo. Detecting anomalies in space using multivariate convolutional lstm with mixtures of probabilistic pca. In Proceedings of the 25th ACM SIGKDD international conference on knowledge discovery & data mining, pages 2123–2133, 2019.
- [Tax and Duin, 2004] David MJ Tax and Robert PW Duin. Support vector data description. *Machine learning*, 54:45–66, 2004.
- [Tolstikhin et al., 2021] Ilya O Tolstikhin, Neil Houlsby, Alexander Kolesnikov, Lucas Beyer, Xiaohua Zhai, Thomas Unterthiner, Jessica Yung, Andreas Steiner, Daniel Keysers, Jakob Uszkoreit, et al. Mlp-mixer: An all-mlp architecture for vision. Advances in neural information processing systems, 34:24261–24272, 2021.

- [Xu et al., 2021] Jiehui Xu, Haixu Wu, Jianmin Wang, and Mingsheng Long. Anomaly Transformer: Time Series Anomaly Detection with Association Discrepancy. 2021.
- [Xu et al., 2022] Hongzuo Xu, Yijie Wang, Songlei Jian, Qing Liao, Yongjun Wang, and Guansong Pang. Calibrated One-class Classification for Unsupervised Time Series Anomaly Detection, 2022.
- [Yairi et al., 2017] Takehisa Yairi, Naoya Takeishi, Tetsuo Oda, Yuta Nakajima, Naoki Nishimura, and Noboru Takata. A data-driven health monitoring method for satellite housekeeping data based on probabilistic clustering and dimensionality reduction. *IEEE Transactions on Aerospace and Electronic Systems*, 53(3):1384–1401, 2017.
- [Yang et al., 2021] Yiyuan Yang, Yi Li, Taojia Zhang, Yan Zhou, and Haifeng Zhang. Early safety warnings for long-distance pipelines: A distributed optical fiber sensor machine learning approach. In *Proceedings of the AAAI Conference on Artificial Intelligence*, volume 35, pages 14991–14999, 2021.
- [Yang et al., 2023] Yiyuan Yang, Chaoli Zhang, Tian Zhou, Qingsong Wen, and Liang Sun. Dcdetector: Dual attention contrastive representation learning for time series anomaly detection. In *Proc. 29th ACM SIGKDD International Conference on Knowledge Discovery & Data Mining (KDD 2023)*, page 3033–3045, 2023.
- [Yeh et al., 2016] Chin-Chia Michael Yeh, Yan Zhu, Liudmila Ulanova, Nurjahan Begum, Yifei Ding, Hoang Anh Dau, Diego Furtado Silva, Abdullah Mueen, and Eamonn Keogh. Matrix profile i: all pairs similarity joins for time series: a unifying view that includes motifs, discords and shapelets. In 2016 IEEE 16th international conference on data mining (ICDM), pages 1317–1322. IEEE, 2016.
- [Zeng et al., 2022] Ailing Zeng, Muxi Chen, Lei Zhang, and Qiang Xu. Are transformers effective for time series forecasting?, 2022.
- [Zhang et al., 2022] Weiqi Zhang, Chen Zhang, and Fugee Tsung. GRELEN: Multivariate Time Series Anomaly Detection from the Perspective of Graph Relational Learning. In *Thirty-First International Joint Conference on Artificial Intelligence*, volume 3, pages 2390–2397, 2022.
- [Zhou *et al.*, 2019] Bin Zhou, Shenghua Liu, Bryan Hooi, Xueqi Cheng, and Jing Ye. Beatgan: Anomalous rhythm detection using adversarially generated time series. In *IJ-CAI*, volume 2019, pages 4433–4439, 2019.
- [Zhou *et al.*, 2022] Hao Zhou, Ke Yu, Xuan Zhang, Guanlin Wu, and Anis Yazidi. Contrastive autoencoder for anomaly detection in multivariate time series. *Information Sciences*, 610:266–280, 2022.
- [Zong et al., 2018] Bo Zong, Qi Song, Martin Renqiang Min, Wei Cheng, Cristian Lumezanu, Daeki Cho, and Haifeng Chen. Deep autoencoding gaussian mixture model for unsupervised anomaly detection. In *Interna*tional conference on learning representations, 2018.

Appendix

This is the appendix of PatchAD: Patch-based MLP-Mixer for Time Series Anomaly Detection.

Datasets

Many publicly available real-world datasets are extensively used in existing methods. We utilize eight datasets to evaluate model performance: (1) MSL (Mars Science Laboratory dataset), (2) SMAP (Soil Moisture Active Passive dataset), (3) PSM (Pooled Server Metrics), (4) SMD (Server Machine Dataset), (5) SWaT (Secure Water Treatment Testbed), (6) WADI (Water Distribution Testbed), (7) NIPS-TS-SWAN, and (8) NIPSTS-GECCO. Table 4 shows the details.

Table 4: Details of benchmark datasets.

Dataset	#Training	#Test (Labeled)	Dimension	Anomaly ratio (%)
SML	58317	73729	55	10.5
SMAP	135183	427617	25	12.8
PSM	132481	87841	25	27.8
SMD	708377	708393	38	4.2
SWaT	99000	89984	26	12.2
WADI	1048571	172801	123	5.99
PS-TS-SWAN	60000	60000	38	32.6
S-TS-GECCO	69260	69261	9	1.1
	SML SMAP PSM SMD SWaT WADI PS-TS-SWAN	SML 58317 SMAP 135183 PSM 132481 SMD 708377 SWaT 99000 WADI 1048571 PS-TS-SWAN 60000	SML 58317 73729 SMAP 135183 427617 PSM 132481 87841 SMD 708377 708393 SWaT 99000 89984 WADI 1048571 172801 PS-TS-SWAN 60000 60000	SML 58317 73729 55 SMAP 135183 427617 25 PSM 132481 87841 25 SMD 708377 708393 38 SWaT 99000 89984 26 WADI 1048571 172801 123 PS-TS-SWAN 60000 60000 38

Baslines

We compared our model against 27 benchmark models, including: (1) Reconstruction-based: AutoEncoder [Sakurada and Yairi, 2014], LSTM-VAE [Park et al., 2018], Omni-Anomaly [Su et al., 2019], BeatGAN [Zhou et al., 2019], InterFusion [Li et al., 2021b]; (2) Autoregression-based: VAR [Anderson, 1976], Autoregression [Rousseeuw and Leroy, 2005], LSTM-RNN [Bontemps et al., 2016], LSTM [Hundman et al., 2018], CL-MPPCA [Tariq et al., 2019]; (3) Density-based: LOF [Breunig et al., 2000], MMPCACD [Yairi et al., 2017], DAGMM [Zong et al., 2018]; (4) Clustering-based: DeepSVDD [Ruff et al., 2018], THOC [Shen et al., 2020], ITAD [Shin et al., 2020]; Matrix Profile [Yeh et al., 2016]; (5) The classic methods: OCSVM [Schölkopf et al., 2001], OCSVM-based subsequence clustering (OCSVM*), IForest [Liu et al., 2008], IForest-based subsequence clustering (IForest*), Gradient boosting regression (GBRT) [Elsayed et al., 2021]; (6) Change point detection and time series segmentation methods: BOCPD [Adams and MacKay, 2007], U-Time [Perslev et al., 2019], TS-CP2 [Deldari et al., 2021]; (7) Transformer-based: Anomaly Transformer ⁷ [Xu et al., 2021]; DCdetector ⁸ [Yang et al., 2023]; These two are current state-of-the-art methods.

Implementation Details

All experiments were conducted using PyTorch implementation on a single NVIDIA GTX 1080TI GPU. We summarize the default hyperparameters of PatchAD as follows: PatchAD consists of 3 encoder layers (L=3). The hidden layer dimension d_{model} is set to 40. The default projector constraint coefficient is 0.2. The Adam optimizer's default learning rate is

 10^{-4} , with a batch size of 128, trained for 3 epochs across all datasets. Different patch sizes and window sizes were chosen for each dataset, defaulting to [3, 5] and 105, respectively. If an anomaly score at any given timestamp exceeds a threshold σ , the model identifies it as an anomaly. The default value for σ is 1. For details on parameter selection, please refer to the Appendix.

Algorithm's Pseudo-code

Algorithm 1 PatchAD's Python-like code

```
PE = PositionEmbedding(d_model) # Postional Embedding
VE_n, VE_p = Linear(dim1, d_model), Linear(dim2, d_model)
# Value Embedding of N and P views
# Patching and Embedding
x_n = rearange(x, 'b (n p) c \rightarrow b c n p', p=patch_size)

x_p = rearange(x, 'b (p n) c \rightarrow b c p n', p=patch_size)
x_n = VE_n(x_n)
x_p = VE_p(x_p)
# x_n's shape (B, c_dim, n_dim, d_model)
# x_p's shape (B, c_dim, p_dim, d_model)
Channel_Mixer = MLP(c_dim, transpose_dim=1)
Inter_Mixer = MLP(n_dim, transpose_dim=2)
Intra_Mixer = MLP(p_dim, transpose_dim=2)
MixRep_Mixer = MLP(d_model, transpose_dim=3)
# Patch Mixer Encoding
x_inter = Channel_Mixer(x_n)
x intra = Channel Mixer(x p)
x_inter = Inter_Mixer(x_inter)
x_intra = Intra_Mixer(x_intra)
x inter = MixRep Mixer(x inter)
x_intra = MixRep_Mixer(x_intra)
# Dual Project
x_inter = x_inter.mean(1)
x_intra = x_intra.mean(1)
Inter_Proj = MLP(d_model)
Intra_Proj = MLP(d_model)
x_inter2 = Inter_Proj(x_inter)
x_intra2 = Intra_Proj(x_intra)
  Ouput shape (B, n_dim, d_model) and (B, p_dim, d_model)
# Upsample to (B, L, d_model)
def loss_fn(a, b):
   return KL(a, b.detach()) + KL(b.detach(), a)
def inter intra loss fn(n, p):
   return loss_fn(n, p) - loss_fn(p, n)
loss1 = inter_intra_loss_fn(x_inter, x_intra)
loss_n_proj = inter_intra_loss_fn(x_inter, x_intra2)
loss_p_proj = inter_intra_loss_fn(x_inter2, x_intra)
loss_proj = loss_n_proj + loss_p_proj
final_loss = (1-c) * loss1 + c * loss_proj
# backward and optimize
```

Full Comparison Results

In Table 5, Aff-P and Aff-R are the precision and recall of affiliation metric [Huet *et al.*, 2022], respectively. R_A_R and R_A_P are Range-AUC-ROC and Range-AUC-PR [Paparrizos *et al.*, 2022], respectively. V_ROC and V_RR are volumes under the surfaces created based on ROC curve and PR curve [Paparrizos *et al.*, 2022], respectively. Besides, we give more results in table 6, and the results from more real-world multivariate time-series datasets show that our proposed PatchAD has good robustness as well as performance.

⁷https://github.com/thuml/Anomaly-Transformer

⁸https://github.com/DAMO-DI-ML/KDD2023-DCdetector

Table 5: Multi-metrics results on all real-world multivariate datasets. All results are in %, the best ones are in **Bold**, and the second ones are underlined.

Dataset	Method	Acc	F 1	Aff-P	Aff-R	R_A_R	R_A_P	V_ROC	V_PR
	AnomalyTrans	98.69	93.93	51.76	95.98	90.04	87.87	88.20	86.26
MSL	DCdetector	98.83	94.77	51.01	96.74	91.29	89.12	89.80	87.81
WISE	PatchAD	98.92	95.02	52.06	96.44	90.89	88.66	90.09	87.99
	AnomalyTrans	99.05	96.41	51.39	98.68	96.32	94.07	95.52	93.37
SMAP	DCdetector	99.06	96.38	50.29	98.04	93.76	92.40	92.70	91.47
	PatchAD	99.15	96.75	52.30	98.70	96.05	94.23	95.12	93.42
	AnomalyTrans	98.68	97.37	55.35	80.28	91.83	93.03	88.71	90.71
PSM	DCdetector	98.81	97.63	52.33	76.95	89.91	91.74	85.57	88.52
1 51.1	PatchAD	98.95	98.11	55.58	82.72	94.85	95.65	<u>89.26</u>	91.67
	AnomalyTrans	99.11	90.06	72.63	98.27	82.12	75.90	81.86	75.69
SMD	DCdetector	98.78	86.02	51.61	93.44	76.13	69.85	73.60	67.45
	PatchAD	98.84	86.62	50.81	93.32	77.55	<u>71.16</u>	74.09	67.88
	AnomalyTrans	98.62	94.62	53.03	98.08	97.89	93.47	97.92	93.49
SWaT	DCdetector	93.25	96.51	52.76	97.33	98.23	95.54	98.25	95.56
	PatchAD	99.12	96.52	52.78	98.17	98.23	95.55	98.26	95.57
	AnomalyTrans	98.17	85.47	87.84	99.75	87.20	78.50	87.36	78.63
WADI	DCdetector	98.70	89.26	59.63	90.98	87.56	81.62	87.16	81.23
	PatchAD	99.06	92.43	60.37	91.76	89.85	84.18	90.68	84.99
	AnomalyTrans	84.57	62.29	58.45	9.49	86.42	93.26	84.81	92.00
NIPS-TS-SWAN	DCdetector	85.99	73.31	38.73	3.13	88.02	94.78	86.02	93.49
	PatchAD	86.05	73.41	51.44	4.34	88.03	94.80	86.13	93.57
	AnomalyTrans	98.26	37.08	55.65	89.12	60.74	28.17	60.48	28.02
NIPS-TS-GECCO	DCdetector	98.57	46.76	49.66	87.68	61.01	32.13	60.77	31.90
	PatchAD	98.64	49.35	53.04	89.48	63.59	35.92	63.09	35.43

 $Table \ 6: \ More \ results \ on \ all \ real-world \ multivariate \ datasets. \ All \ results \ are \ in \ \%, \ the \ best \ ones \ are \ in \ \textbf{Bold}, \ and \ the \ second \ ones \ are \ \underline{underlined}.$

Dataset		MSL			SMAP			PSM			SMD			SWaT		Average
Metric	P	R	F1	F1												
LOF	47.72	85.25	61.18	58.93	56.33	57.60	57.89	90.49	70.61	56.34	39.86	46.68	72.15	65.43	68.62	60.94
OCSVM	59.78	86.87	70.82	53.85	59.07	56.34	62.75	80.89	70.67	44.34	76.72	56.19	45.39	49.22	47.23	60.25
U-Time	57.20	71.66	63.62	49.71	56.18	52.75	82.85	79.34	81.06	65.95	74.75	70.07	46.20	87.94	60.58	65.62
IForest	53.94	86.54	66.45	52.39	59.07	55.53	76.09	92.45	83.48	42.31	73.29	53.64	49.29	44.95	47.02	61.22
DAGMM	89.60	63.93	74.62	86.45	56.73	68.51	93.49	70.03	80.08	67.30	49.89	57.30	89.92	57.84	70.40	70.18
ITAD	69.44	84.09	76.07	82.42	66.89	73.85	72.80	64.02	68.13	86.22	73.71	79.48	63.13	52.08	57.08	70.92
VAR	74.68	81.42	77.90	81.38	53.88	64.83	90.71	83.82	87.13	78.35	70.26	74.08	81.59	60.29	69.34	74.66
MMPCACD	81.42	61.31	69.95	88.61	75.84	81.73	76.26	78.35	77.29	71.20	79.28	75.02	82.52	68.29	74.73	75.74
CL-MPPCA	73.71	88.54	80.44	86.13	63.16	72.88	56.02	99.93	71.80	82.36	76.07	79.09	76.78	81.50	79.07	76.66
TS-CP2	86.45	68.48	76.42	87.65	83.18	85.36	82.67	78.16	80.35	87.42	66.25	75.38	81.23	74.10	77.50	79.00
Deep-SVDD	91.92	76.63	83.58	89.93	56.02	69.04	95.41	86.49	90.73	78.54	79.67	79.10	80.42	84.45	82.39	80.97
BOCPD	80.32	87.20	83.62	84.65	85.85	85.24	80.22	75.33	77.70	70.90	82.04	76.07	89.46	70.75	79.01	80.33
LSTM-VAE	85.49	79.94	82.62	92.20	67.75	78.10	73.62	89.92	80.96	75.76	90.08	82.30	76.00	89.50	82.20	81.24
BeatGAN	89.75	85.42	87.53	92.38	55.85	69.61	90.30	93.84	92.04	72.90	84.09	78.10	64.01	87.46	73.92	80.24
LSTM	85.45	82.50	83.95	89.41	78.13	83.39	76.93	89.64	82.80	78.55	85.28	81.78	86.15	83.27	84.69	83.32
OmniAnomaly	89.02	86.37	87.67	92.49	81.99	86.92	88.39	74.46	80.83	83.68	86.82	85.22	81.42	84.30	82.83	84.69
InterFusion	81.28	92.70	86.62	89.77	88.52	89.14	83.61	83.45	83.52	87.02	85.43	86.22	80.59	85.58	83.01	85.70
THOC	88.45	90.97	89.69	92.06	89.34	90.68	88.14	90.99	89.54	79.76	90.95	84.99	83.94	86.36	85.13	88.01
AnomalyTrans	91.92	96.03	93.93	93.59	99.41	96.41	96.94	97.81	97.37	84.14	96.88	90.06	89.79	100.0	94.62	94.48
DCdetector	92.22	97.48	94.77	94.43	98.41	96.38	97.19	98.08	97.63	83.04	89.22	86.02	93.25	100.0	96.51	94.26
PatchAD	92.05	98.20	95.02	94.49	99.13	96.75	97.72	98.52	98.11	83.06	90.51	86.62	93.28	100.0	96.52	94.60

Table 7: Parameter studies on project head constraint results (patch size=[3,5], window size=105). All results are in %.

Dataset		M	SL			SM	IAP			PS	SM	
Contraint	Acc	P	R	F1	Acc	P	R	F1	Acc	P	R	F1
0.0	98.51	91.67	94.49	93.06	99.01	93.55	99.05	96.22	98.73	97.42	98.03	97.72
0.1	98.92	91.96	98.33	95.03	99.04	94.43	98.33	96.34	98.72	97.35	98.04	97.70
0.2	98.92	92.05	98.20	95.02	99.11	94.42	98.91	96.61	98.91	97.43	98.66	98.04
0.3	98.89	92.03	97.93	94.88	99.14	94.41	99.11	96.71	98.89	97.42	98.59	98.00
0.4	98.86	92.09	97.54	94.73	99.12	94.45	98.97	96.66	98.71	97.42	97.94	97.68
0.5	98.96	92.12	98.60	95.25	99.02	94.40	98.17	96.25	98.73	97.42	98.03	97.72
0.6	98.92	92.11	98.20	95.06	99.01	94.39	98.07	96.19	98.92	97.45	98.70	98.07
0.7	98.84	91.91	97.59	94.67	99.07	94.43	98.55	96.44	98.76	97.39	98.14	97.76
0.8	98.91	92.01	98.20	95.00	99.10	94.40	98.81	96.55	98.92	97.42	98.73	98.07
0.9	98.78	91.99	96.90	94.38	98.96	94.37	97.70	96.01	98.92	97.47	98.64	98.05

Table 8: Parameter studies on anomaly threshold σ results (patch size=[3,5], window size=105). All results are in %.

Dataset		M	SL			SM	AP			PS	SM	
AR	Acc	P	R	F1	Acc	P	R	F1	Acc	P	R	F1
0.5	97.93	95.39	84.39	89.55	99.15	96.46	96.91	96.68	98.45	98.61	95.77	97.17
0.6	98.27	94.70	88.54	91.52	99.15	95.84	97.58	96.70	98.77	98.33	97.20	97.76
0.7	98.17	93.76	88.54	91.07	99.09	95.22	97.77	96.48	98.70	98.07	97.20	97.64
0.8	98.45	93.19	92.04	92.61	99.15	94.73	98.86	96.75	98.95	97.94	98.29	98.11
0.9	98.45	92.36	92.93	92.64	99.01	94.07	98.49	96.23	98.92	97.68	98.45	98.06
1.0	98.84	91.80	97.73	94.67	99.01	94.05	98.49	96.22	98.70	97.30	98.03	97.66
1.1	98.73	91.22	97.36	94.19	98.85	92.76	98.69	95.63	98.68	97.06	98.20	97.63
1.2	98.64	90.45	97.36	93.78	98.76	92.19	98.69	95.33	98.62	96.85	98.20	97.52

Table 9: Parameter studies on d_{model} size results (patch size=[3,5], window size=105). All results are in %.

Dataset		M	SL			SM	IAP			PS	SM	
$\overline{d_{model}}$	Acc	P	R	F1	Acc	P	R	F1	Acc	P	R	F1
10	98.62	91.81	95.42	93.58	99.04	94.42	98.28	96.31	98.87	97.38	98.56	97.97
20	98.92	92.08	98.20	95.04	98.98	94.33	97.88	96.07	98.73	97.37	98.05	97.71
30	98.89	92.06	97.94	94.91	99.10	94.43	98.80	96.57	98.87	97.43	98.52	97.97
40	98.91	92.03	98.20	95.02	99.13	94.49	98.95	96.67	98.73	97.42	98.03	97.72
50	98.93	92.15	98.20	95.08	99.11	94.45	98.89	96.62	98.90	97.44	98.63	98.03
60	98.91	92.03	98.20	95.02	99.13	94.44	98.98	96.66	98.94	97.48	98.74	98.10
70	98.87	92.08	97.67	94.79	99.05	94.40	98.43	96.37	98.97	97.48	98.83	98.15
80	98.77	91.99	96.70	94.29	99.03	94.38	98.24	96.27	98.89	97.44	98.58	98.00
90	98.92	92.06	98.20	95.03	99.05	94.38	98.42	96.35	98.89	97.46	98.56	98.01

Table 10: Parameter studies on encoder layers L results (patch size=[3,5], window size=105). All results are in %.

Dataset		M	SL			SM	AP		PSM				
Encoder layer	Acc	P	R	F1	Acc	P	R	F1	Acc	P	R	F1	
1	98.60	91.72	95.27	93.46	98.76	94.29	96.11	95.19	98.10	97.28	95.82	96.54	
2	98.88	91.96	97.93	94.85	99.01	94.42	98.09	96.22	98.79	97.44	98.20	97.82	
3	98.92	92.07	98.20	95.03	99.10	94.41	98.79	96.55	98.84	97.47	98.36	97.91	
4	98.88	92.19	97.67	94.85	99.11	94.42	98.91	96.61	98.95	97.41	98.83	98.12	
5	98.83	91.95	97.41	94.60	99.13	94.46	99.02	96.69	98.87	97.44	98.52	97.98	

Table 11: Parameter studies on window size results (window size=105). All results are in %.

Dataset		M	SL			SM	[AP		PSM				
Window size	Acc	P	R	F1	Acc	P	R	F1	Acc	P	R	F1	
30	98.11	91.47	90.52	90.99	98.91	94.38	97.23	95.78	98.88	97.48	98.51	97.99	
45	97.98	91.23	89.44	90.33	98.93	95.55	96.14	95.84	98.67	97.30	97.92	97.61	
60	98.33	92.05	92.16	92.10	98.86	94.18	97.09	95.62	98.75	97.59	97.93	97.76	
75	98.51	91.79	94.31	93.03	98.93	94.27	97.60	95.90	98.72	97.35	98.06	97.70	
90	98.71	91.92	96.24	94.03	99.06	94.34	98.55	96.40	98.92	97.44	98.71	98.07	
105	98.92	92.05	98.20	95.02	99.08	94.44	98.60	96.48	98.66	97.38	97.79	97.59	
120	98.86	92.10	97.55	94.75	99.13	94.47	98.98	96.67	98.79	97.53	98.13	97.83	
135	98.65	91.85	95.67	93.72	99.07	94.46	98.50	96.44	98.88	97.38	98.60	97.99	
150	98.71	91.83	96.30	94.02	99.12	94.48	98.91	96.64	98.66	97.43	97.72	97.58	
165	98.61	91.85	95.27	93.53	99.09	94.50	98.65	96.53	98.73	97.44	97.98	97.71	
180	98.53	91.73	94.55	93.12	99.01	94.35	98.18	96.23	98.70	97.55	97.78	97.66	
195	98.77	92.02	96.70	94.31	98.96	94.35	97.74	96.01	98.87	97.44	98.50	97.97	
210	98.81	91.97	97.17	94.50	98.83	94.30	96.71	95.49	98.92	97.45	98.69	98.06	

Table 12: Parameter studies on multi-scale patch size results (window size=105). All results are in %.

Dataset		M	SL			SM	[AP		PSM				
Patch size	Acc	P	R	F1	Acc	P	R	F1	Acc	P	R	F1	
[1]	98.49	91.73	94.12	92.91	99.09	94.47	98.69	96.53	98.66	97.21	97.99	97.60	
[3]	98.57	91.67	95.08	93.34	99.08	94.44	98.61	96.48	98.84	97.56	98.26	97.91	
[5]	98.34	91.70	92.66	92.18	99.02	94.40	98.20	96.26	98.83	97.44	98.37	97.91	
[7]	98.45	91.96	93.41	92.68	99.13	94.46	99.04	96.70	98.88	97.43	98.56	97.99	
[1, 3]	98.63	91.87	95.42	93.61	99.11	94.48	98.86	96.62	98.78	97.46	98.16	97.81	
[1, 5]	98.63	91.88	95.42	93.61	99.07	94.43	98.58	96.46	98.72	97.37	98.04	97.70	
[1, 7]	98.63	91.89	95.42	93.62	99.04	94.43	98.32	96.33	98.71	97.39	97.99	97.69	
[3, 5]	98.78	91.99	96.90	94.38	99.07	94.39	98.63	96.46	98.91	97.43	98.66	98.04	
[3, 7]	98.68	91.92	95.93	93.88	99.09	94.40	98.76	96.53	98.87	97.41	98.55	97.97	
[5, 7]	98.61	91.86	95.27	93.53	99.08	94.44	98.63	96.49	98.85	97.40	98.46	97.93	
[1, 3, 5]	98.85	92.01	97.54	94.69	99.12	94.47	98.92	96.64	98.82	97.37	98.39	97.88	
[1, 3, 7]	98.74	92.00	96.46	94.18	99.09	94.40	98.71	96.50	98.79	97.43	98.21	97.82	
[1, 5, 7]	98.92	92.05	98.20	95.02	99.04	94.38	98.36	96.33	98.67	97.36	97.87	97.61	
[3, 5, 7]	98.56	91.76	94.89	93.30	99.08	94.42	98.61	96.46	98.87	97.45	98.52	97.98	
[1, 3, 5, 7]	98.62	91.78	95.42	93.56	99.08	94.43	98.61	96.48	98.92	97.43	98.71	98.06	